

Cell manipulation using magnetic nanowires

A. Hultgren and M. Tanase

Department of Physics and Astronomy, Johns Hopkins University, Baltimore, Maryland 21218

C. S. Chen

Department of Biomedical Engineering, Johns Hopkins University, Baltimore, Maryland 21218

G. J. Meyer

Departments of Chemistry and Materials Science and Engineering, Johns Hopkins University, Baltimore, Maryland 21218

D. H. Reich^{a)}

Department of Physics and Astronomy, Johns Hopkins University, Baltimore, Maryland 21218

(Presented on 14 November 2002)

The use of magnetic nanowires is demonstrated as a method for the application of force to mammalian cells. Magnetic separations were carried out on populations of NIH-3T3 mouse fibroblast cells using ferromagnetic Ni wires 350 nm in diameter and 35 μm long. Separation purities in excess of 90% and yields of 49% are obtained. The nanowires are shown to outperform magnetic beads of comparable volume. © 2003 American Institute of Physics.

[DOI: 10.1063/1.1556204]

Magnetic nanoparticles are finding an ever-increasing range of applications in biology and medicine, from force transduction,^{1,2} to cancer therapy,³ and biosensing.⁴ One new type of magnetic particle with considerable potential for use in this rapidly growing field of biomagnetics are electrodeposited magnetic nanowires.^{5,6} These wires are fabricated by electrochemical deposition in nanoporous templates, a process that permits detailed control of their morphology, composition, and magnetic properties. The magnetic and electrical properties of these structures have been widely studied,^{7–10} but their potential for biotechnology uses is largely untapped.

One of the most widespread uses of magnetic nanoparticles in biological systems is in magnetic cell separation.^{1,11–14} In this article, we describe cell separation experiments using ferromagnetic nickel nanowires, demonstrating that electrodeposited nanowires can also be used to apply forces on mammalian cells. We compare the results of separation using nanowires and commercially available “magnetic beads,” the most common magnetic nanoparticle used in separations. We find that the wires outperform the beads, both in purity and yield of the separated cell populations.

The nickel nanowires used in this study were made in the nanopores of 50- μm -thick alumina filter templates (Anodisc, Whatman, Inc.) using a method described previously.¹⁵ Nanowires grown from these templates have an average diameter of 350 ± 40 nm. For this study, we used wires grown to a length of $l = 35$ μm . The nanowires were released from the template by dissolving the alumina in warm KOH, and then washed with water and sterilized in 70% ethanol. An example of a nanowire is shown in Fig. 1(a). While in suspension, the nanowires were magnetized parallel to their

long axis by exposure to magnetic fields in excess of 1 kG. The magnetic beads used for comparison were polystyrene spheres with diameter 1–2 μm , containing dispersed single-domain $\gamma\text{-Fe}_2\text{O}_3$ nanoparticles at 20 vol % (Polysciences, Inc.). This structure gives the beads a superparamagnetic behavior.¹⁶ A scanning electron microscope image of two beads is shown in Fig. 1(b). Note that the volume of a nanowire is equal to that of a 1.8 μm diameter bead.

The field dependence on the magnetic moment of the nanowires and beads was measured with a vibrating sample magnetometer. The nanowires cannot be accurately measured in the alumina templates because the high pore density of $3 \times 10^8/\text{cm}^2$ results in significant dipolar interactions between the wires.^{17,18} Therefore, a 1000 \times more dilute sample of nanowires was prepared by suspending 2×10^5 wires in 0.5 mL of epoxy (Araldite 502). The epoxy was cured in a 2 kG magnetic field to keep the nanowires aligned. A sample of beads was prepared by air-drying 2.4×10^8 beads on a glass cover slip. The normalized room-temperature magnetization curves, M vs H , for the wires and beads are shown in Fig. 2. The beads show no remnance and a saturation magnetization of $M_S = 32$ emu/cm³, slightly lower but consistent with the value $M_S = 35$ –45 emu/cm³ specified by the manufacturer. The magnetization of the nickel nanowires along the

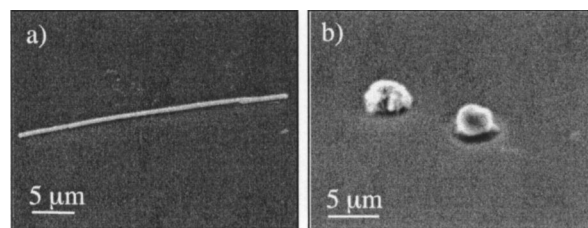


FIG. 1. Scanning electron micrograph of (a) a 35 μm long Ni nanowire, and (b) 2 μm diameter superparamagnetic beads.

^{a)}Electronic mail: dhr@pha.jhu.edu

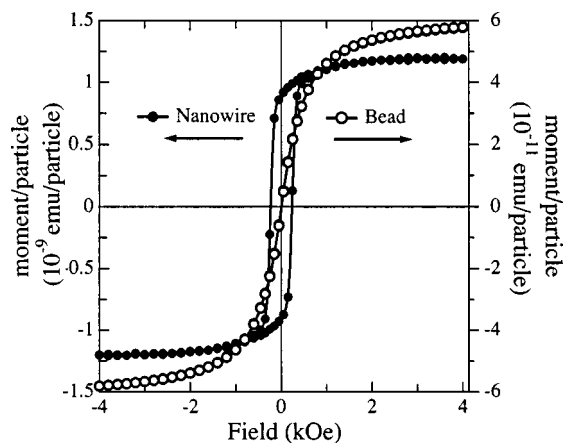


FIG. 2. Magnetic moment vs field for superparamagnetic beads and $35\ \mu\text{m}$ ferromagnetic nickel nanowires.

easy axis was found to be $M_S \approx 415\ \text{emu}/\text{cm}^3$, with a remnant magnetization $M_R = 0.8M_S$. One possible source of the somewhat lower value of M_S compared to the bulk value of nickel is oxidation of a surface layer of the nanowires due to exposure to KOH during removal from the templates.

The cells used for magnetic separations were NIH-3T3 mouse fibroblasts, cultured in high glucose Dulbecco's Modified Eagle Medium (Gibco Life Sciences) supplemented with antibiotics and 5% calf serum. The cells were grown to areal densities ranging from 60 to $210/\text{mm}^2$. To attach the particles to the cells, the nanowires and beads were first suspended in sterile $1\times$ phosphate buffered saline solution (PBS) at a concentration of 60 000 particles/mL, then sonicated for 5 min to reduce aggregation, and introduced into the culture dishes at particle to cell ratios $<1:3$. These low particle concentrations reduced the binding of multiple particles to single cells, allowing us to avoid the effects of particle concentration and to study the behavior of individual particles. The cells have an affinity for binding to hydrophilic surfaces such as the native nickel oxide layer on the nanowires and carboxylate groups on the beads.¹⁹ These interactions are mediated by the extracellular matrix proteins present in the calf serum. After a 24 h incubation period ($37\ ^\circ\text{C}$, 5% CO_2) with the magnetic particles, the cells remained bound to the beads and wires even when dissociated from the culture dishes in trypsin EDTA. Also, when trypsinized cells bound to particles were replated into culture dishes, they adhered to the surface of the dish normally and proliferated at a rate comparable to cells which had not been exposed to magnetic material. This indicates that the particles are not immediately toxic to the cells.

The magnetic separations were done in 1 cm diameter glass test tubes with two rare earth magnets positioned on opposite sides of the tube. The magnets produced a face field of 0.4 T and an average field gradient of 80 T/m inside the separator. A 5 min exposure to these magnets is sufficient to complete the separation. To perform a separation, cells with magnetic particles attached were trypsinized and suspended in fresh culture medium. Half of the cells were immediately replated and used to determine the fraction of cells bound to magnetic particles at the start of the separation. This corrects

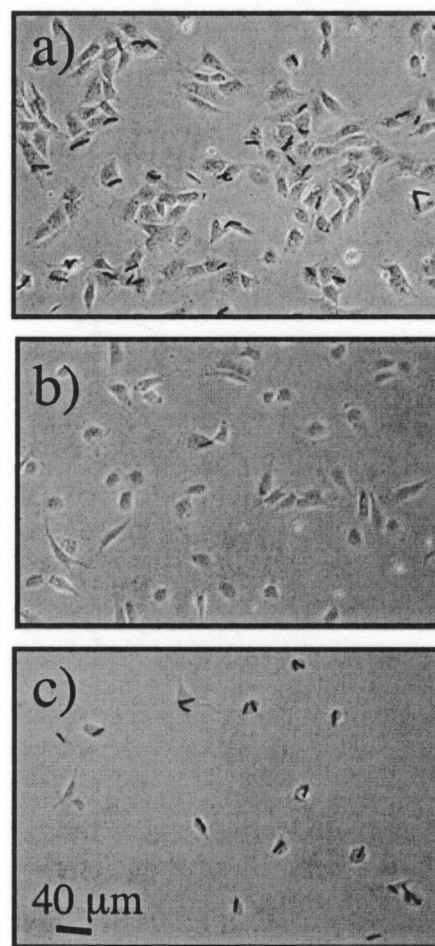


FIG. 3. Optical micrographs of cell populations in a magnetic separation using $35\ \mu\text{m}$ nanowires. (a) Initial cell population after incubation with nanowires; (b) cells not captured during magnetic separation; (c) cells captured during separation. Each image is a superposition of a phase contrast micrograph that images the cells, and a bright field micrograph that images the wires. The nanowires are visible as dark lines on the cells.

for any potential losses of cells or detachment of the magnetic particles during trypsinization. The remaining cells were then introduced into the magnetic separator. After separation, the suspended cells not captured by the magnets were extracted from the separator and plated into a culture dish. The magnets were then removed and the cells that had been captured were resuspended in culture medium and plated as well. All three populations were then incubated for 1 h to allow the cells to settle and adhere to the dishes. In addition to these single-pass separations, we also carried out three-pass separations to increase the purity of the separated cell populations. For these triple separations, the separated cells were run through the above procedure two additional times before replating.

Cell counting was done over a $16\ \text{mm}^2$ area of each sample, using images acquired with the $10\times$ objective of a Nikon TS100 tissue culture microscope equipped with a CoolPix995 digital camera. At this magnification, the nanowires and beads that are bound to the cells are difficult to observe in phase-contrast images against the background of cell organelles. However, they are readily seen in bright field

TABLE I. % efficiency and yield for magnetic separations.

Type of magnetic particle	Number of separations	% of captured cells with particles	% of uncaptured cells with particles	% yield
Nanowire	1	80±7%	6±1%	49±3%
	3	94±4%	2±0.5%	29±1%
Beads	1	46±6%	2±0.2%	19±2%
	3	85±5%	2±0.6%	15±3%

images where the cells are not visible. An accurate determination of which cells contain magnetic particles was made by superimposing images of these two types.

Examples of cell populations from this study are shown in Fig. 3. Figure 3(a) shows cells prior to separation with 11% of the cells bound to nanowires. Figure 3(b) shows uncaptured cells. Only 1 of 57 of these cells contains a nanowire. Figure 3(c) shows the magnetically captured cells. Nanowires are visible in 9 of 12 of these cells. As suggested by these images, the nanowires are very effective at separating bound from unbound cells. Quantitative results for both single and triple separations for the wires and the beads are shown in Table I. Each result is averaged over three runs, normalized to the cell density in the dish. One important measure of the effectiveness of magnetic separation is the purity of the resulting cell populations. For single separations with wires, we find that 80% of the captured cells contain nanowires, while 94% of the uncaptured cells do not contain wires. With the three step separations, the captured purity rises to 94% and the uncaptured purity to 98%. We also find that the nanowires produce purer cell populations than the beads. Our measured captured cell purity for one-pass separations done with the beads is nearly a factor of two lower than for the nanowires. The nanowires retain their advantage in three-pass separations as well.

Another figure of merit for separations is the yield, namely the fraction of the initial population of the cells of interest that are captured. Since we have only one cell type in our experiment, we define yield as the ratio of the number of captured cells with magnetic material divided by the number of initial cells with magnetic material. As shown in Table I, the yield in a single separation is nearly 50% for the nanowires, more than two times higher than for the beads. This advantage is retained in three-pass separations, although unlike the purity, the yield for both wires and beads decreases with increasing number of separation passes, due to losses introduced by repeated manipulation of the cells.

These experiments have demonstrated that electrodeposited ferromagnetic nanowires can be used to apply forces to

mammalian cells. We have shown that the essential mechanics of cell separation—binding and physical manipulation—work well with magnetic nanowires, and that high purity and yield are obtainable. In addition, the 35 μm nanowires we tested outperform magnetic beads of comparable volume at low particle-to-cell concentrations. Part of the increased efficiency of the nanowires over the beads tested may be attributable to their larger magnetic moment, but their larger surface area may also make them bind more effectively to the cells. Further experiments, including characterization of the separation efficiency on nanowire size and composition, and the development of surface functionalization techniques to control wire–cell interactions will be required to fully explore the capabilities of magnetic nanowires for applications of this type.

This work was supported by DARPA/AFOSR Grant No. F49620-02-1-0307 and by the David and Lucile Packard Foundation through Grant No. 2001-17715. VSM measurements were made using central facilities supported by the JHU MRSEC under NSF Grant No. DMR-0080031.

- ¹I. Safarik and M. Safarikova, *J. Chromatogr., B: Biomed. Appl.* **722**, 33 (1999).
- ²F. C. MacKintosh and C. F. Schmidt, *Colloids Surf.* **4**, 300 (1999).
- ³*Scientific and Clinical Applications of Magnetic Microspheres*, edited by U. Häfeli, W. Schütt, J. Teller, and M. Zborowski (Plenum, New York, 1997).
- ⁴D. R. Baselt, G. L. Lee, M. Natesan, S. W. Metzger, P. E. Sheehan, and R. J. Colton, *Biosens. Bioelectron.* **13**, 731 (1998).
- ⁵A. Fert and L. Piraux, *J. Magn. Magn. Mater.* **200**, 338 (1999).
- ⁶M. Lederman, R. O'Barr, and S. Schultz, *IEEE Trans. Magn.* **31**, 3793 (1995).
- ⁷M. Zheng, R. Skomski, Y. Liu, and D. J. Sellmyer, *J. Phys.: Condens. Matter* **12**, L497 (2000).
- ⁸K. Ounadjela, R. Ferré, L. Louail, J. M. George, J. L. Maurice, L. Piraux, and S. Dubois, *J. Appl. Phys.* **81**, 5455 (1997).
- ⁹C. Beeli, B. Doudin, J. Ph. Ansermet, and P. Stadelmann, *J. Magn. Magn. Mater.* **164**, 77 (1996).
- ¹⁰P. A. Smith, C. D. Nordquist, T. N. Jackson, T. S. Mayer, B. R. Martin, J. Mbindyo, and T. E. Mallouk, *Appl. Phys. Lett.* **77**, 1399 (2000).
- ¹¹C. Bergemann, D. Müller-Schulte, J. Oster, L. à Brassard, and A. S. Lübke, *J. Magn. Magn. Mater.* **194**, 45 (1999).
- ¹²K. Rudi, F. Larsen, and K. S. Jakobsen, *Appl. Environ. Microbiol.* **64**, 34 (1998).
- ¹³K. W. Peasley, *Med. Hypotheses* **46**, 5 (1996).
- ¹⁴L. R. Moore, M. Zborowski, L. Sun, and J. J. Chalmers, *J. Biochem. Biophys. Methods* **37**, 11 (1998).
- ¹⁵M. Tanase, L. A. Bauer, A. Hultgren, D. M. Silevitch, L. Sun, D. H. Reich, P. C. Searson, and G. J. Meyer, *Nano Lett.* **1**, 155 (2001).
- ¹⁶J. K. Vassiliou, V. Mehrotra, J. W. Otto, and N. R. Dollahon, *Mater. Sci. Forum* **225**, 725 (1996).
- ¹⁷A. Encinas-Oropesa, M. Demand, L. Piraux, U. Ebels, and I. Huynen, *J. Appl. Phys.* **89**, 6704 (2001).
- ¹⁸L. Cheng-Zhang and J. C. Lodder, *J. Magn. Magn. Mater.* **88**, 236 (1990).
- ¹⁹Polysciences, Inc., Technical data sheet 438.